CHIN. PHYS. LETT. Vol. 33, No. 11 (2016) 113202

Excitation Dependence of Dipole–Dipole Broadening in Selective Reflection Spectroscopy *

Teng-Fei Meng(孟腾飞)[1,2], Zhong-Hua Ji(姬中华)[1,2], Yan-Ting Zhao(赵延霆)[1,2**], Lian-Tuan Xiao(肖连团)[1,2], Suo-Tang Jia(贾锁堂)[1,2]

[1]*State Key Laboratory of Quantum Optics and Quantum Optics Devices, Institute of Laser Spectroscopy, Shanxi University, Taiyuan 030006*

[2]*Collaborative Innovation Center of Extreme Optics, Shanxi University, Taiyuan 030006*

(Received 2 September 2016)

We investigate the dipole–dipole broadened selective reflection spectrum with the Cs atomic density of 10^{14}–10^{15} cm^{-3}. The dipole–dipole broadening is reduced and the hyperfine splitting is well resolved when the ground state atoms are excited by a detuned pump beam. The dependences of dipole–dipole broadening of Cs atoms in the $6S_{1/2}(F=3) \rightarrow 6P_{3/2}(F'=4)$ hyperfine transition line on atomic density and the excitation factor are studied. It is found that the reduction of the dipole–dipole broadening is dependent on the pump beam power and is independent of the atomic density in this density range. These results are useful for understanding of the dynamical process in this range of atomic density.

PACS: 32.70.Jz, 42.50.Ct, 34.80.Dp DOI: 10.1088/0256-307X/33/11/113202

For many applications and fundamental physics it is necessary to know the nonlinear optical response of an atomic gas when dipole–dipole interactions can not be ignored. The dipole–dipole interaction[1,2] can modify the radiative decay rate[3] and can induce a splitting or shift of the resonance.[4] The study of dipole–dipole interaction is useful for astrophysics, plasma physics, especially the study of a variety of nonlinear optical phenomena in dense atomic vapors, such as lasers without inversion,[5] optical bistability,[6] electromagnetically induced transparency,[7] four-wave mixing[8,9] and self-induced transparency.[10]

The dipole–dipole interaction can be studied in selective reflection spectrum at gas–solid surface because it has simple setup and high resolution spectrum.[11] When the atomic density is very low (less than 10^{13} cm^{-3}), the Doppler effect dominates the lineshape. The broadening caused by the dipole–dipole interaction can be ignored.[12] In the range of 10^{16}–10^{17} cm^{-3} the resonant dipole–dipole interaction dominates the lineshape. The corresponding broadening is known as self-broadening or resonance broadening.[13–15] By using a cw pump-probe technique, the excitation dependence of the dipole–dipole broadening has been observed in rubidium[16] and potassium[17] vapors. The linewidth is narrowed effectively with fine splitting resolved by the pump beam. The experimental results can be interpreted by the classic dielectric function[18,19] and the Fresnel formula. For the atoms in the range of 10^{14}–10^{15} cm^{-3}, which are often used in quantum coherence[11,12,20–23] and dynamic process,[24,25] the dipole–dipole broadening is comparable with the Doppler broadening and cannot be ignored. It allows for hyperfine resolution as the Doppler broadening is less than the hyperfine splitting if we can eliminate the dipole–dipole broadening. However, there are few works about theory and experiment of selective reflection (SR) spectral lineshapes for atomic gases at this density.

In the present work, we investigate the SR spectrum in the density range of 10^{14}–10^{15} cm^{-3}. The results are analyzed by the Liouville equation.[26] We study the dipole–dipole broadening of Cs atoms in the $6S_{1/2}(F=3) \rightarrow 6P_{3/2}(F'=4)$ hyperfine transition line in the presence and in the absence of a detuned pump beam. The excitation dependences of dipole–dipole broadening on the pump power and the atomic density are investigated.

The SR spectra can be interpreted in terms of the probe reflection coefficient of atomic vapor. At normal incidence, the reflection coefficient R of a two-level atomic system is given as[27]

$$R = \left(\frac{n-1}{n+1}\right)^2 + \frac{4n(n-1)}{(n+1)^3}\mathrm{Re}T, \tag{1}$$

where n is the real refractive index of a dielectric, and ReT is the real part of dimensionless quantity T and will be presented in detail in the following.

For excitation of the atoms caused by a pump beam, there are two additional items which are added to our theory model: (i) the dipole–dipole interaction between ground and excited state atoms, and (ii) the nonresonant excitation of atoms by a pump beam.

*Supported by the National Basic Research Program of China under Grant No 2012CB921603, the National Natural Science Foundation of China under Grant Nos 61275209, 11304189, 61378015 and 11434007, the Shanxi Scholarship Council of China, and the Program for Changjiang Scholars and Innovative Research Team in Universities of China under Grant No IRT13076.

**Corresponding author. Email: zhaoyt@sxu.edu.cn

© 2016 Chinese Physical Society and IOP Publishing Ltd

Then ReT can be expressed as

$$\mathrm{Re}T = \frac{\hbar\eta N\Omega_\mathrm{s}}{4\varepsilon_0 E_\mathrm{s}^2}\phi, \tag{2}$$

where $\hbar$ is the reduced Planck constant, N is the density of atoms, Ω_s is the Rabi frequency of the probe beam, ε_0 is the permittivity of vacuum, E_s is the amplitude of the probe beam, ϕ is a dimensionless factor, and η is the fractional population difference between the ground and excited states[28,29] and can be expressed as

$$\eta = \frac{N_\mathrm{g} - (N_\mathrm{e} + N_\mathrm{ne})(2F_\mathrm{g}+1)/(2F_\mathrm{e}+1)}{N}, \tag{3}$$

where N_g is the density of ground state atoms, N_e and N_ne are the atomic density of excited state caused by the resonant probe beam and the detuned pump beam, respectively, $\eta = 1$ corresponds to zero excitation, $\eta = 0$ corresponds to maximum excitation, F_g and F_e are the total atomic angular momentum quantum numbers of the ground and excited states, respectively.

The dimensionless quantity ϕ is the sum of the dimensionless quantities ϕ_+ and ϕ_-, which are defined as

$$\begin{aligned}\phi_+ &= -\,\mathrm{Re}\int_0^{+\infty} W(v_z)(-2ik_\mathrm{s})\widehat{\sigma}_{21}(-2ik_\mathrm{s}, v_z)dv_z,\\ \phi_- &= -\,\mathrm{Re}\int_{-\infty}^{0} W(v_z)\overline{\sigma}_{21}(v_z)dv_z,\end{aligned} \tag{4}$$

where ϕ_+ represents the contribution to the SR from atoms with positive velocities (after collision with surface). Similarly, ϕ_- represents the contribution from atoms with negative velocities (before collision with surface), $W(v_z)$ is a normalized Maxwell–Boltzmann distribution function (v_z is the atomic velocity in the z-direction), σ_{21} is the density matrix element of reduced density matrix σ, and $\widehat{\sigma}_{21}$ is obtained by the Laplace transformation of σ_{21}. The subscripts 2 and 1 denote excited and ground state levels, respectively. Here $\overline{\sigma}_{21}$ is the stationary value of σ_{21}, and $\widehat{\sigma}_{21}$ and $\overline{\sigma}_{21}$ can be obtained by the Liouville equation

$$\begin{aligned}\widehat{\sigma}_{21}(v_z, p) = \frac{i\Omega_\mathrm{s}(v_z p + \Gamma_2)}{2p}&\{v_z p + i(\Delta_\mathrm{s} - k_\mathrm{s}v_z)\\ &+ \gamma_{21}\}/\{(v_z p + \Gamma_2)[(v_z p + \gamma_{21})^2\\ &+ (\Delta_\mathrm{s} - k_\mathrm{s}v)^2] + (vp + \gamma_{21})\Omega_\mathrm{s}^2\},\end{aligned} \tag{5}$$

and

$$\overline{\sigma}_{21}(v_z) = \frac{i\Omega_\mathrm{s}\Gamma_2}{2}\frac{i(\Delta_\mathrm{s} - k_\mathrm{s}v_z) + \gamma_{21}}{\Gamma_2[\gamma_{21}^2 + (\Delta_\mathrm{s} - k_\mathrm{s}v)^2] + \gamma_{21}\Omega_\mathrm{s}^2}, \tag{6}$$

where γ_{21} can be expressed as $\gamma_{21} = \frac{1}{2}\Gamma_2 + \Gamma_\mathrm{d}$, with Γ_d being the dipole–dipole broadening expressed as[13]

$$\Gamma_\mathrm{d} = f r_\mathrm{e}\lambda_0 c\eta N[(2F_\mathrm{g}+1)(2F_\mathrm{e}+1)]^{1/2}. \tag{7}$$

The experimental setup and the relevant hyperfine structure energy levels of Cs are shown in Fig. 1. The probe field excites the $6S_{1/2}(F = 3)$ state to the $6P_{3/2}(F' = 2, 3, 4)$ state. The corresponding power is small enough (less than 10 μW), thus no saturation effects need to be considered. The frequency of pump beam is tuned to be 5.6 GHz below the $6S_{1/2}(F = 3) \to 6P_{3/2}(F' = 4)$ transition to avoid resonant excitation. The pump power is up to 300 mW. The two beams are linearly polarized and are sent to the window at a near-normal incident angle (0.02 rad). The probe beam is overlapped with the pump beam at a spot with diameter $d = 0.3$ mm on the interface between the Cs vapor and the window. To achieve sufficient density of atoms, the vapor cell is installed in an oven. The temperature of the Cs vapor is 177℃–216℃, and the corresponding atomic density is 6.7×10^{14}–2.85×10^{15} cm^{-3}. The outside surface windows are slightly wedged to separate the reflections from two surfaces.

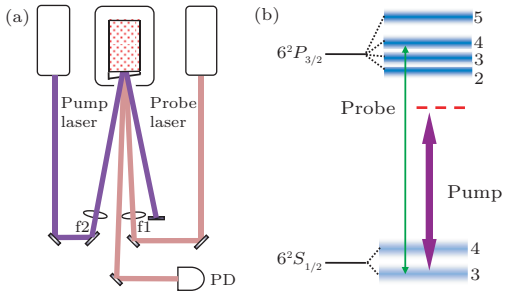

Fig. 1. (Color online) The experimental setup (a) and energy diagram of the D2 line of Cs (b). Pump and probe laser beams are focused on the interface between Cs vapor and window. The reflection is recorded by a photodetector.

Figure 2 shows the SR spectra as a function of the probe laser frequency. The probe laser frequency is scanned over 5 GHz around the $6S_{1/2}(F = 3) \to 6P_{3/2}$ transition. The blue curve is the saturated absorption spectroscopy (SAS) for the frequency reference. The black solid curve is the SR signal in the absence of the pump beam. The corresponding temperature of the cell is 208℃, and the atomic density N is 2.16×10^{15} cm^{-3}. In the presence of the pump beam with a power of 300 mW, the width and amplitude of SR signal decrease, as shown by the red solid curve. The decrease is caused by the nonresonant excitation of the ground state atoms by the pump beam.

We use Eq. (2) to fit SR signal with the spectral width Γ and the excitation factor η as fitting parameters. The excitation factor η is normalized to 1 for the case when the pump beam is absent. The green dashed curve is the fitting result when the pump beam is absent after considering the three reflection lines arising from the $6S_{1/2}(F = 3) \to 6P_{3/2}(F' = 2, 3, 4)$ transition. We can see that the dip near −500 MHz in the horizontal axis has deviation from the experimental curve. It is caused by the reduced destructive

interference between reflection of surface and atoms in the experiment. In fact, a similar degree of destructive interference has been observed in thin cells, which can be controlled by the wave vector, dressing field and cell length.[30] Other parts are in good agreement with the spectrum obtained in the experiment. The dipole–dipole broadening is derived from the curve when $R > 0$, thus this deviation of simulation does not influence the result of dipole–dipole broadening.

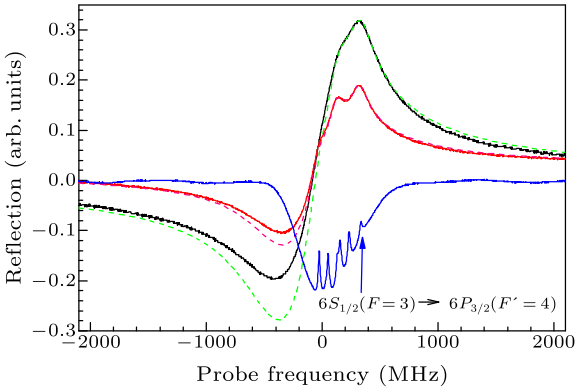

Fig. 2. (Color online) SR spectrum at atomic density $N = 2.16 \times 10^{15}\,\mathrm{cm}^{-3}$. Black and red solid curves correspond to the cases without and with the pump laser ($P = 300\,\mathrm{mW}$), respectively. Green and pink dashed curves are the corresponding simulated results. Blue solid curve is the referenced SAS.

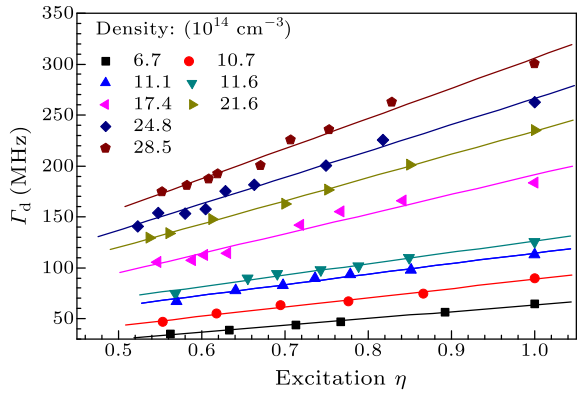

Fig. 3. (Color online) The fitting value of the width plotted as a function of the excitation factor η. Different symbols represent the results at different atomic densities from $N = 6.7 \times 10^{14}$ to $N = 2.85 \times 10^{15}\,\mathrm{cm}^{-3}$. The straight lines are the linear fitting.

The spectrum of the $6S_{1/2}(F = 3) \rightarrow 6P_{3/2}(F' = 4)$ transition is used to analyze the dipole–dipole broadening in the following. The fitting width is 348 MHz and $\eta = 1$. The pink dashed curve is the fitting SR signal in the presence of pump beam. The fitting width is 242 MHz and $\eta = 0.54$. The dipole–dipole broadening Γ_d in high density range is obtained based on the measured value of the SR spectrum in low density range and calculated value of Doppler broadening. The detailed process is described in the following. The spectral linewidth of this transition is measured to be 102 MHz at the temperature of around 120℃ ($2 \times 10^{13}\,\mathrm{cm}^{-3}$), where Γ_d can be ignored due to the low atomic density,[12] thus it can be regarded as the Doppler broadening Γ_D at this temperature. Based on the relation between the Doppler broadening and temperature T, $\Gamma_D \propto \sqrt{T}$, the Doppler broadening in high atomic density can be calculated. When the temperature is 208℃, the Doppler broadening is calculated to be 113 MHz. As the spectral width mainly contains the dipole–dipole broadening and the Doppler broadening, the dipole–dipole broadenings are derived to be 235 MHz and 129 MHz in the absence and presence of the pump beam, respectively.

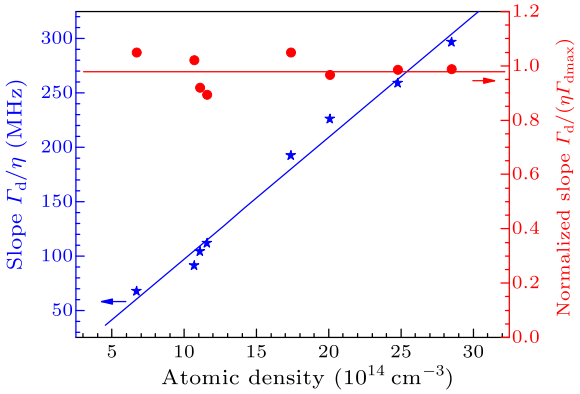

Fig. 4. (Color online) The dependence of the slope and the normalized slope on the atomic density. The blue line is a linear fitting of the slope. The red line is the value of the normalized slope.

We change the pump power to obtain the SR spectra while keeping the atomic density invariable. The fitting of these SR signals gives the widths and the corresponding excitation factors. The results are shown as the magenta triangle ($N = 2.16 \times 10^{15}\,\mathrm{cm}^{-3}$) in Fig. 3, where the width is plotted as a function of the excitation factor η. The magenta line is the corresponding linear fitting. The width increases linearly with the excitation factor η. It is coincided with Eq. (7). Then we measure the widths and the excitation factors at different atomic densities from $N = 6.7 \times 10^{14}\,\mathrm{cm}^{-3}$ to $N = 2.85 \times 10^{15}\,\mathrm{cm}^{-3}$, which are also shown in Fig. 3. The slopes with different atomic densities are summarized in Fig. 4, labeled by stars. It can be seen that the slope increases with the atomic density. The solid line in Fig. 4 is a linear fitting, which is in agreement with Eq. (7). Further, the normalized slopes, which are defined as the ratio of the slope to the width without the pump laser, are also shown in Fig. 4, labeled by solid circle. The average value of the normalized slope is 0.98 ± 0.05, which shows that there is no variation for the normalized slope. For $\eta = 1$ we have $\Gamma_d = \Gamma_{dmax} = f r_e \lambda_0 c N[(2F_g+1)(2F_e+1)]^{1/2}$. We obtain that the normalized slope equals to $\frac{\Gamma_d}{\eta}\frac{1}{\Gamma_{dmax}} = 1$. Thus the normalized slope is in agreement with the

theoretical value. This result reflects that the narrowing of dipole–dipole broadening is dependent on the pump power and independent of the temperature. Thus the strong excitation dependence of the self-broadened width can be interpreted by using the quasistatic model of the dipole–dipole interaction in the density range of 10^{14}–$10^{15}\,\mathrm{cm}^{-3}$.

In conclusion, the SR spectra of the $6S_{1/2}(F = 3) \rightarrow 6P_{3/2}(F' = 4)$ hyperfine transition of Cs with a red detuning pump beam have been studied in the range of atomic density from 6.7×10^{14}–$2.85 \times 10^{15}\,\mathrm{cm}^{-3}$. The dipole–dipole broadening and excitation factor are obtained by numerical fitting. The dipole–dipole broadening increases linearly with the excitation factor for different atomic densities. The normalized slope is independent of the density. These results can be interpreted by using the quasistatic model of the dipole–dipole interactions, and can help us to understand the cavity quantum electrodynamics mechanism, which have potential applications in high precision measurements and achieving better optoelectronic devices.

References

[1] Cheng M T, Ma X S and Wang X 2014 *Chin. Phys. Lett.* **31** 014202
[2] Altiere E, Fahey D P, Noel M W, Smith R J and Carroll T J 2011 *Phys. Rev.* A **84** 053431
[3] DeVoe R G and Brewer R G 1996 *Phys. Rev. Lett.* **76** 2049
[4] Hettich C, Schmitt C, Zitzmann J, Kühn S, Gerhardt I and Sandoghdar V 2002 *Science* **298** 385
[5] Manka A S, Dowling J P, Bowden C M and Fleischhauer M 1994 *Phys. Rev. Lett.* **73** 1789
[6] Malyshev A V 2012 *Phys. Rev.* A **86** 065804
[7] Xu Z X, Qu W Z, Gao R, Hu X H and Xiao Y H 2013 *Chin. Phys.* B **22** 033202
[8] Zhang Y P, Khadka U, Anderson B and Xiao M 2009 *Phys. Rev. Lett.* **102** 013601
[9] Zhang Y P, Wang Z G, Nie Z Q, Li C B, Chen H X, Lu K Q and Xiao M 2011 *Phys. Rev. Lett.* **106** 093904
[10] Stroud C R and Bowden C M 1988 *Opt. Commun.* **67** 387
[11] Badalyan A, Chaltykyan V, Grigoryan G, Papoyana A, Shmavonyan S and Movsessian M 2006 *Eur. Phys. J.* D **37** 157
[12] Keaveney J 2013 *PhD Dissertation: Cooperative Interactions in Dense Thermal Rb Vapour Confined in nm-Scale Cells* (Durham: Durham University)
[13] Lewis E L 1980 *Phys. Rep.* **58** 1
[14] Leegwater J A and Mukamel S 1994 *Phys. Rev.* A **49** 146
[15] Niemax K, Movre M and Pichler G 1979 *J. Phys.* B **12** 3503
[16] Li H, Varzhapetyan T S, Sautenkov V A, Rostovtsev Y V, Chen H, Sarkisyan D and Scully M O 2008 *Appl. Phys.* B **91** 229
[17] Kampen H V, Sautenkov V A, Smeets C J C, Eliel E R and Woerdman J P 1999 *Phys. Rev.* A **59** 271
[18] Maki J J, Malcuit M S, Sipe J E and Boyd R W 1991 *Phys. Rev. Lett.* **67** 972
[19] Maki J J, Davis W V, Boyd R W and Sipe J E 1992 *Phys. Rev.* A **46** 7155
[20] Thomas R J 2012 *PhD Dissertation: Observation and Characterization of Electromagnetically Induced Transparency Using Evanescent Fields* (Calgary: University of Calgary)
[21] Simmons Z J, Proite N A, Miles J, Sikes D E and Yavuz D D 2012 *Phys. Rev.* A **85** 053810
[22] Zhao J M, Zhao Y T, Wang L R, Xiao L T and Jia S T 2002 *Appl. Phys.* B **75** 553
[23] Zhao Y T, Ma J, Wang L R, Zhao J M, Xiao L T and Jia S T 2005 *J. Phys.* B **38** 3037
[24] Kondo R, Tojo S, Fujimoto T and Hasuo M 2006 *Phys. Rev.* A **73** 062504
[25] Weller L, Bettles R J, Siddons P, Adams C S and Hughes I G 2011 *J. Phys.* B **44** 195006
[26] Schuller F, Gorceix O and Ducloy M 1993 *Phys. Rev.* A **47** 519
[27] Nienhuis G, Schuller F and Ducloy M 1988 *Phys. Rev.* A **38** 5197
[28] Manassah J T 1983 *Phys. Rep.* **101** 359
[29] Friedberg R, Hartmann S R and Manassah J T 1973 *Phys. Rep.* **7** 101
[30] Li C B, Zhang Y P, Wang Z G, Li Y Y, Nie Z Q, Zhao Y, Wang R M, Yuan C Z and Lu K Q 2011 *Opt. Commun.* **284** 1379